Macromolecular Research, Vol. 14, No. 5, pp 499-503 (2006)

SALS Study on Transcrystallization and Fiber Orientation in Glass Fiber/Polypropylene Composites

Kun Na

Division of Biotechnology, The Catholic University of Korea, Bucheon 420-743, Korea

Han Soo Park, Hong Youn Won, Jong Kwan Lee, and Kwang Hee Lee*

Center for Advanced Functional Polymers, Department of Polymer Science and Engineering, Inha University, Incheon 402-751, Korea

Joo Young Nam

Functional Materials Group, Central R&D Center, Dongwoo Fine-chem Co. Ltd., Gyeonggi-do 451-764, Korea

Byung Suk Jin

Department of Applied Chemistry, College of Pharmacy, Dongduk Women's University, Seoul 136-714, Korea

Received March 18, 2006; Revised June 23, 2006

Abstract: This report presents a new technical approach for evaluating the fiber orientation of composites using small-angle light scattering (SALS). Glass fiber (GF)/polypropylene (PP) composites with different fiber orientations were prepared by drawing compression-molded specimens. The drawn samples were remelted and then annealed at 150 °C in order to induce a crystalline structure on the fiber surface, and then underwent SALS analysis. The samples showed a combination of circular and streak patterns. The model calculations demonstrated that the number of nuclei on the fiber surface and the thickness of the transcrystalline layer affected the sharpness and intensity of the streak pattern. In addition, the azimuthal angle of the streak pattern was found to be dependent on the direction of the transcrystalline layer, which correlated with the fiber direction. This correlation suggests that the fiber orientation in the composites can be easily evaluated using SALS.

Keywords: composite, fiber orientation, small-angle light scattering, transcrystallization.

Introduction

The mechanical properties of polypropylene (PP) are improved by reinforcing them with glass fibers (GF). When molding the GF/PP composite parts, the fibers will tend to orient in different directions. This orientation improves mechanical properties in the fiber direction while diminishing in the transverse direction. If fiber orientation can be determined, and thus controlled, the designer can optimize the geometry and process to produce a light weight and lower cost product.[1-3] Under certain conditions, the fiber surface provides a large number of nucleation sites for crystallization. This means that lamellar crystals grow from the fiber surface in the radial direction only, producing a cylindrical layer of crystals, which are known as transcrystalline. It is well known that the crystalline morphology and the orientation of the reinforced fiber have a large influence on the properties of composites.[4-6] However, to our knowledge, these two phenomena have only been studied separately. When the PP/GF composite films are stretched, the fibers become oriented at the stretching direction. For stretched samples, it is expected that the fiber orientation and the crystalline morphology may be strongly coupled. In this study, a correlation was established between the transcrystalline structure on the fiber surface and its corresponding small-angle light scattering (SALS) pattern. More specifically, a correlation was established between the fiber direction and the azimuthal angle of the streak pattern, which suggests a new scattering technique for evaluating the average fiber orientation in the composites.

*Corresponding Author. E-mail: polylee@inha.ac.kr

Experimental

Commercial PP (PP186, MI=60) produced by Honam Petrochemical Co. (Korea) was used. The chopped GF sized for PP was supplied by Owens Coring Korea (CS04-147A). The fiber length and diameter were 4 mm and 10 μm,

respectively.

The undrawn GF/PP composite films were prepared as follows. GF were randomly dispersed between the PP films and compression-molded at 200 °C for 10 min. After molding, the samples were quenched in ice water. Dumbbell-type specimens with a size of $0.15 \times 40 \times 10$ mm^3 were cut and stretched using a Hounsfield universal testing machine equipped with a heating chamber. Uniaxial stretching was carried out at 140 °C with a strain rate of 2 mm/min. The actual draw ratio was determined from the displacement of an ink mark made on the specimens, which was 5 mm apart prior to stretching. After stretching, the specimens were remelted at 200 °C for 5 min and then annealed at 150 °C for 2 hr in order to induce a transcrystalline structure on the fiber surface. Pre-oriented samples were also prepared via compression molding. In that case, continuous GF strands were used.

The H_v light scattering patterns were obtained using a polarized He-Ne gas laser with a 632.8 nm wavelength. The light was polarized in the vertical direction, while the optical axis of the analyzer was set horizontally. The H_v light scattering pattern was recorded using a highly sensitive CCD camera. Polarizing microscopic observations were carried out using an OLYMPUS-BX50.

Results and Discussion

Figure 1 shows optical micrographs of the pre-oriented GF/PP composites with an isothermal crystallization time. A typical transcrystalline layer with a sheaf shape developed on the fiber surface. The lamellar crystals are believed to initially overgrow from rows of nucleating points in a direction normal to the fiber surface. The growth front occasionally branches at some distances and angles in space into new lamellae, leading to the development of a diverging sheaf of fibrils. The sheaves are aligned almost side by side with their axes preferentially oriented parallel to the fiber axis. The thickness of the transcrystalline layer and the nucleation density on the fiber surface increases with increasing crystallization time. It should be noted that the spherulites grown in the PP matrix exist alongside the transcrystalline layer for isothermal crystallization.

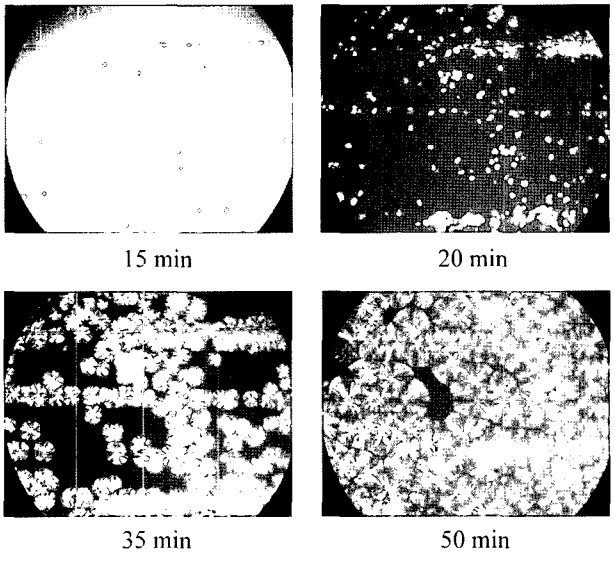

Figure 1. Optical micrographs of the GF/PP composites at various crystallization time.

Figure 2 shows typical H_v light scattering patterns from the specimen whose direction of the fiber axis was set to -45 °C to the direction of polarizer. Both an azimuthally dependent four-leaf pattern and streak pattern are observed for all specimens. The angular position of the broad-leaf patterns shifts to a lower angle region with increasing time. This suggests that the size of the spherulite in the PP matrix increases with increasing crystallization time. On the other hand, the weak streak pattern at an azimuthal angle of 45 ° appeared early in the experiment and became sharper with increasing time. The observed sharp streak pattern might be due to the increased thickness of the transcrystalline layers.

A theoretical approach to the light scattering patterns was made in order to further understand the streak patterns. The scattering equation for this system is similar to that previously reported by other researchers[7,8] for a stacked sheaflike texture, as shown in Figure 3.

According to the method proposed by Blundell,[9] the nor-

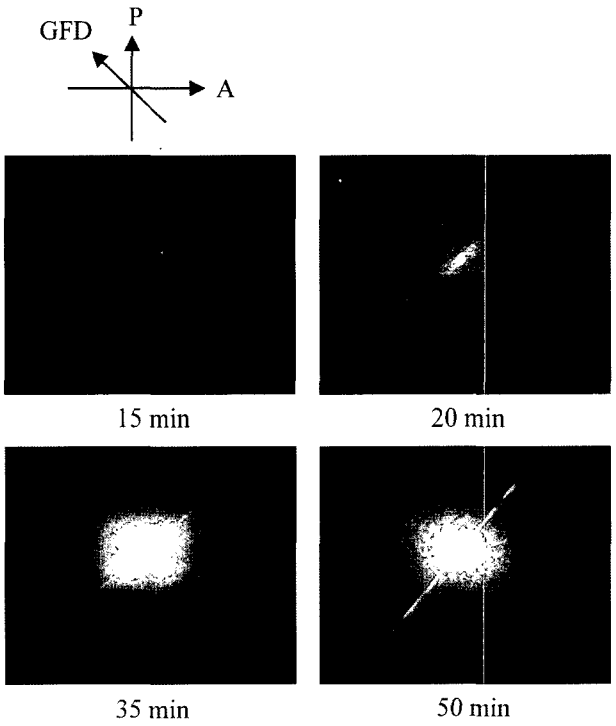

Figure 2. H_v light scattering patterns of the GF/PP composites at various crystallization times. Direction of the GF (GFD) was set to -45 ° against the polarizer direction (P).

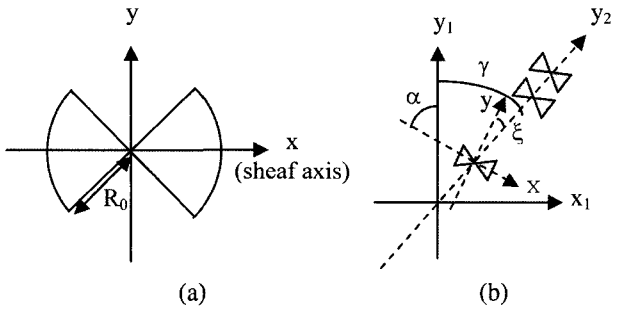

Figure 3. Model used for the theoretical analysis of the light scattering intensity distribution. (a) Optically anisotropic sector as a model for the sheaflike crystalline superstructure and (b) relationship between the sheaf and stack of the sheaf.

malized scattering intensity from an assembly of the sheaves in given by

$$I_{Hv} = Re\left\{\langle|f|^2\rangle - |\langle f\rangle|^2 + \frac{1+F_x}{1-F_x}|\langle f\rangle|^2\right\} - Re\left\{\frac{2|\langle f\rangle|^2 F_x(1-F_x^N)}{N(1-F_x)^2}\right\} \quad (1)$$

where

$$F_x = |F|\exp[-2\pi i \sin\theta\cos(\mu-\gamma)X/\lambda] \quad (2)$$

$$|F| = \exp[-2\pi^2\sin^2\theta\cos^2(\mu-\gamma)\sigma_x^2 X/\lambda^2] \quad (3)$$

where μ, θ, and γ are the azimuthal, scattering and particular angles, respectively. X is the long period, N is number of sheaves in the stack and λ is the wavelength of light in a vacuum. Eq. (1) is the same formulation given by Hosemann and Bagchi[10] in the case when the fluctuation of the domain thickness has no correlation with the statistics of the lattice. The term $\langle|f|^2\rangle - |\langle f\rangle|^2$ represents the diffuse background scattering of a generally weak intensity, which arises from orientation fluctuations of individual sheaves and the distribution of the sheaf size. The term $Re\{(1+F_x)/(1-F_x)\}$ corresponds to the reciprocal lattice factor, which converges to unity with increasing scattering angle θ. If there is no orientation fluctuation and all sheaves are the same size, the total scattered field $f(h)$ is as follows[7]:

$$f(h) = R_0(M\cdot O)\times\int_0^{R_0} r dr \exp(ih\cdot r) \quad (4)$$

where R_0 is the radius of the sector and $(M\cdot O)$ is the scattering power per unit area under H_v polarization conditions, which is given by

$$(M\cdot O) = \frac{\delta_0}{2}\cos\rho_2\sin\{2(\xi+\omega-\gamma)\}E_0 \quad (5)$$

In this formula, δ_0 is the anisotropy of the scattering element defined by α_1-α_2, which is assumed to be uniaxially symmetrical with polarizabilities α_1 and α_2 along and perpendicular to the optical axis. ω is the polar angle between the optical axis and the sheaf axis and E_0 is the amplitude of an incident beam. If there is no fluctuation in orientation, i.e. $\xi=\xi_0$, ξ_0, $\cos\rho_2$ is defined using the equation reported by Clough *et al.*[11] as follows:

$$\cos\rho_2 = \frac{\cos\theta}{\sqrt{\cos^2\theta+\sin^2\theta\sin^2\mu}} \quad (6)$$

The H_v scattering intensity I_{sp} of spherulite is theoretically described as follows[12-15]:

$$I_{sp} = AV^2\cos^2\rho_2(3/U^3)^2\{(\alpha_r-\alpha_t) \times [\cos^2(\theta/2)/\cos\theta]\cos^2\mu(4\sin U - U\cos U - 3SiU)\}^2 \quad (7)$$

where A is the proportionality factor, V is the volume of spherulites with radius R, μ is the azimuthal angle, and α_r and α_t are the radial and tangential polarizabilities of the spherulite, respectively. SiU is the sine integral defined as

$$SiU = \int_0^U (\sin x/x)dx \quad (8)$$

where U is given by

$$U = 4\pi(R/\lambda)\sin(\theta/2) \quad (9)$$

In this study, total intensity of both spherulite and the transcrystalline layer was calculated by a convolution of eqs. (1) and (7). The numerical calculations were carried out assuming that the optical axis formed a polar angle ω=0 with respect to the sheaf axis, and the sheaf had the same size, i.e. there were no size fluctuations.

Figure 4 shows the patterns calculated, in which the values of all parameters except for R_0, and X were fixed. In order to simplify the analysis for the calculated patterns, the parameter describing the spherulite radius was set to 10 μm, and the parameter describing the fluctuation in the identity period was fixed to a very small value such as σ_x/X=0.001. The parameter associated with the orientation angle of the stacks was fixed at γ=-45° because the tilt angle of the fiber axis in Figure 2 was set to -45°. All the patterns showed a streak at μ=45°. This streak pattern appeared at R_0=5 μm and became sharper with increasing R_0. The high order peak of the streaks also appeared at a large R_0. The sharpness of the streak pattern increased with increasing X. In the composites, the thickness of the transcrystalline layer and distance between the nuclei were assigned to R_0 and X, respectively. This suggests that the number of nuclei on the fiber surface and the thickness of the transcrystalline layer affect the sharpness and intensity of the streak pattern. These results agree with the optical micrographs and H_v scattering patterns shown in

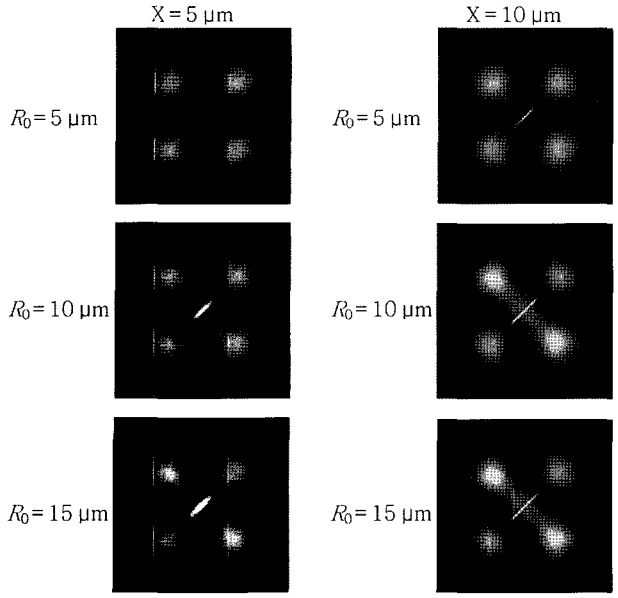

Figure 4. Calculated H_v light scattering patterns by varying X and R_0.

Figures 1 and 2.

Figure 5 shows the patterns calculated at R_0=15 μm and X=5 μm. The model calculation was carried out in order to determine the effect of the spherulite radius, R, and the orientation of the sheaf stack. The maximum scattering angle of the cloverleaf patterns was shifted to lower angle with increasing R. On the other hand, in the case of γ=-10°, the streak patterns appear at μ=10 and 190°, and in the case of γ=-20°, the patterns show the streaks at μ=20 and 200°. This suggests that the azimuthal angle of the streaks concerning the orientation of the stack of sheaflike texture in the specimen is related to the orientation of the fiber axis.

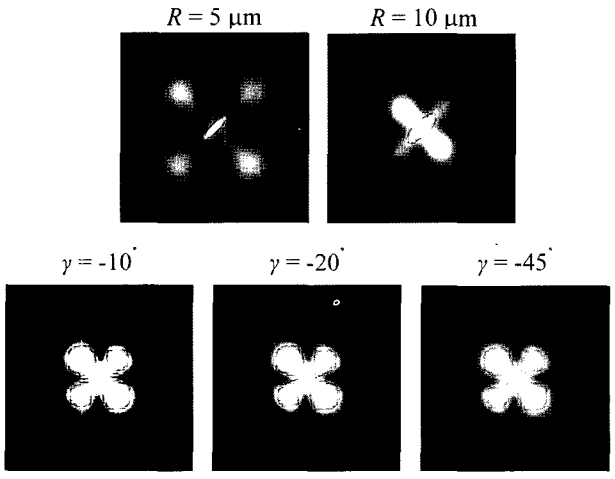

Figure 5. Calculated H_v light scattering patterns by varying R and γ.

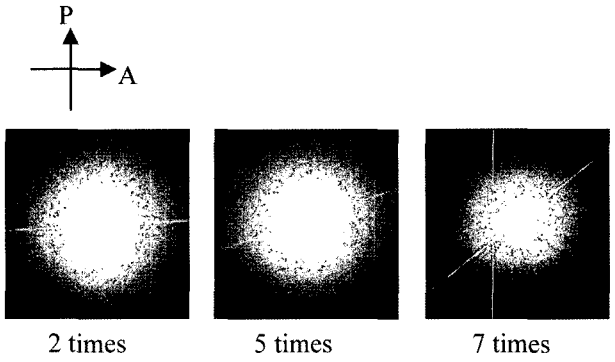

Figure 6. H_v light scattering patterns as a function of the draw ratio.

SALS measurements were carried out for the drawn samples with different fiber orientations in order to examine the relationship between the fiber orientation and the azimuthal angle of the streak pattern. Figure 6 shows the light scattering patterns of the samples stretched at a draw ratio of 2, 5, and 7. The scattering shows the superposition of a circular pattern and a streak pattern. The circular pattern suggests that the glass fibers in the PP matrix spatially restrict the growth of the crystals and favor the random arrangement of the individual lamellar crystallites. The classical clover pattern with zero intensity in the center represents the ideal, best developed spherulite, while the circularly symmetric pattern does not represent a unique morphological situation. Therefore, it was impossible to examine the morphological properties using such circular patterns. It is noting that the azimuthal angle of the streak patterns increased with increasing draw ratio. For the sample with the draw ratio of 7, the azimuthal angle of the streak patterns was close to 45 and 225°, implying that the fibers are well aligned to the machine direction. This indicates that the average fiber orientation of the drawn samples may be related to the azimuthal angle of the streak pattern.[16-18] On the basis of the simulation and experimental results, it is found that the fiber orientation in the composites can be easily evaluated by analyzing the light scattering patterns.

Conclusions

This study examined the correlation between the fiber orientation and the light scattering pattern using the GF/PP composites as a model system. The results showed that streak patterns appeared in SALS as the transcrystalline structure developed on the fiber surface. The number of nuclei on the fiber surface and the thickness of the transcrystalline layer had a large influence on the sharpness and intensity of the streak pattern. The azimuthal angle of the streak patterns increased with increasing fiber orientation. For example, the azimuthal angle of the streak patterns was close to 45 and

225° for a fully oriented sample A comparison between the experimental data and the model calculations suggests that SALS might be used to evaluate the fiber orientation in the composites.

Acknowledgements. This research was supported by grant No. 34318-01 from the National Nuclear R&D Programs of the Ministry of Science & Technology (MOST) of Korea.

References

(1) Y. Zhang, R. Chen, and Z. Hui, *J. Adh. Sci. Tech.*, **14**, 1405 (2000).
(2) S. J. Son, Y. M. Lee, and S. S. Im, *J. Mater. Sci.*, **35**, 5767 (2000).
(3) C. Roux, J. Denault, and M. F. Champagne, *J. Appl. Polym. Sci.*, **78**, 2047 (2000).
(4) C. K. Moon, Y. S. Um, H. H. Cho, J. O. Lee, and T. W. Park, *Polymer (Korea)*, **14**, 630 (1990).
(5) C. K. Moon and Y. S. Um, *Polymer (Korea)*, **15**, 289 (1991).
(6) J. Y. Nam, S. H. Park, K. H. Lee, and J. K. Kim, *Polymer (Korea)*, **27**, 299 (2003).
(7) T. Hashimoto, A. Todo, and H. Kawai, *Polym. J.*, **10**, 521 (1978).
(8) C. Sawatari, M. Iida, and M. Matsuo, *Macromolecules*, **17**, 1765 (1984).
(9) D. Blundell, *Acta Crystallogr.; Sect. A*, **A26**, 472 (1970).
(10) R. Hosemann and S. N. Bagchi, *Direct Analysis of Diffraction by Matter*, North-Holland Publishing Co., Amsterdam, 1962.
(11) S. Clough, J. Van Aartsen, and R. S. Stein, *J. Appl. Polym. Sci.*, **36**, 3072 (1965).
(12) R. S. Stein, A. Misra, T. Yuasa, and F. Khambatta, *Pure Appl. Chem.*, **49**, 915 (1977).
(13) Meeten, *Optical Properties of Polymers*, Elsevier Applied Science Publishers, London, 1986.
(14) C. H. Lee, H. Saito, and T. Inoue, *Macromolecules*, **28**, 8096 (1995).
(15) J. Y. Nam, S. Kadomatsu, H. Saito, and T. Inoue, *Polymer*, **43**, 2101 (2002).
(16) G. Xian, L. Shen, and X. Yi, *Cailiao Yanjiu Xuebao*, **13**, 509 (1999).
(17) W. Yang and G. Dai, *Huadong Ligong Daxue Xuebao*, **24**, 675 (1998).
(18) S. Nagae, T. Otsuka, M. Nishida, T. Shimizu, T. Takeda, and S. Yumitori, *J. Mater. Sci. Let.*, **14**, 1234 (1995).